Title

Network dynamics predict improvement in working memory performance following donepezil administration in healthy young adults

Permalink

https://escholarship.org/uc/item/0jz25680

Authors

Reches, A
Laufer, I
Ziv, K
et al.

Publication Date

2014-03-01

DOI

10.1016/j.neuroimage.2013.11.020

Peer reviewed

Network dynamics predict improvement in working memory performance following donepezil administration in healthy young adults

A. Reches[a,*], **I. Laufer**[a], **K. Ziv**[a], **G. Cukierman**[a], **K. McEvoy**[b], **M. Ettinger**[a], **R.T. Knight**[c,d], **A. Gazzaley**[e], and **A.B. Geva**[a,f]

[a]ElMindA Ltd., Herzliya, Israel

[b]University of California, Los Angeles School of Medicine, Los Angeles, CA, USA

[c]Helen Wills Neuroscience Institute, University of California, Berkeley, CA, USA

[d]Department of Psychology, University of California, Berkeley, CA, USA

[e]Departments of Neurology, Physiology and Psychiatry, University of California San Francisco, San Francisco, CA, USA

[f]Electrical and Computer Engineering, Ben Gurion University of the Negev, Beer Sheba, Israel

Abstract

Attentional selection in the context of goal-directed behavior involves top-down modulation to enhance the contrast between relevant and irrelevant stimuli via enhancement and suppression of sensory cortical activity. Acetylcholine (ACh) is believed to be involved mechanistically in such attention processes. The objective of the current study was to examine the effects of donepezil, a cholinesterase inhibitor that increases synaptic levels of ACh, on the relationship between performance and network dynamics during a visual working memory (WM) task involving relevant and irrelevant stimuli. Electroencephalogram (EEG) activity was recorded in 14 healthy young adults while they performed a selective face/scene working memory task. Each participant received either placebo or donepezil (5 mg, orally) on two different visits in a double-blinded study. To investigate the effects of donepezil on brain network dynamics we utilized a novel EEG-based Brain Network Activation (BNA) analysis method that isolates location–time–frequency interrelations among event-related potential (ERP) peaks and extracts condition-specific networks. The activation level of the network modulated by donepezil, reflected in terms of the degree of its dynamical organization, was positively correlated with WM performance. Further analyses revealed that the frontal–posterior theta–alpha sub-network comprised the critical regions whose activation level correlated with beneficial effects on cognitive performance. These results indicate that condition-specific EEG network analysis could potentially serve to predict beneficial effects of therapeutic treatment in working memory.

*Corresponding author at: Haminhara 16 St., Herzliya 46586, Israel. Fax: +972 9 9516477. amit@elminda.com (A. Reches).

Introduction

Goal-directed attentional selection involves top-down modulation that enhances the contrast between relevant and irrelevant stimuli through enhancement and suppression processes, respectively (Chadick and Gazzaley, 2011; Gazzaley et al., 2005; Labrenz et al., 2012; Zanto et al., 2011). Previous findings suggest that acetylcholine (ACh) is involved in this neural modulation process (Sarter et al., 2005).

Cholinergic input contributes to biasing the processing of stimuli in the parietal cortex (Broussard, 2012). Specifically, it has been suggested that distractors induce increases in prefrontal ACh that in turn recruits parietal ACh efflux to enhance the signal-to-noise ratio (SNR) of relevant signals (see a review in Broussard, 2012).

Donepezil increases cholinergic synaptic transmission in the brain by reducing the activity of the enzyme that breaks down ACh, thereby prolonging the effective life time of this neurotransmitter in the synaptic cleft. Donepezil slightly improves cognitive performance in some mild to moderate Alzheimer's disease (AD) (Birks, 2006). However, there is limited data on either the cognitive or neural impact of donepezil administered to healthy individuals (e.g. Zaninotto et al., 2009). Donepezil has been found to improve retention of training related to executive functions as well as verbal, visual and episodic memory probably through its effects on attention (Husain and Mehta, 2011; Palmer, 2002; Rokem et al., 2010; Rowan et al., 2007; Sarter and Bruno, 1997; Wesnes et al., 2002, 2005). It was also found that donepezil augments the effects of voluntary visual spatial attention (Rokem et al., 2010) that counteract impairments caused by distractors (Roberts and Thiele, 2008; Zenger et al., 2000) and modulates orientation-specific surround suppression (Kosovicheva et al., 2012).

Recent studies have endorsed a network-level approach to examine neural markers of attention processes (Hamker, 2005; Montijn et al., 2012), as well as the neural basis of cognitive enhancers on the brain (Husain and Mehta, 2011; Pa et al., 2013). For example, distributed networks were demonstrated in power and coherence studies involving alpha and theta oscillations during different stages of WM(Bastiaansen et al., 2002; Sauseng et al., 2002, 2004, 2005a, 2005b). Moreover, alpha-theta connectivity was found to be impaired in AD, possibly indicating diminished modulation of activity in the posterior cortices by the frontal cortex (Yener and Ba ar, 2010).

Cross-frequency phase synchronization between the frontal theta and modality-specific posterior alpha oscillations (parietal alpha in the case of visual processing) suggests a role of this double frequency coupling in gating relevant information (Kawasaki et al., 2010) and is in agreement with findings in the literature emphasizing the importance of phase synchronization in memory processes (Fell and Axmacher, 2011). This proposed frontal–posterior theta–alpha network is also in line with previous findings demonstrating oscillatory mechanisms of visual WM over a distributed network implicating prefrontal, occipitoparietal

and medial temporal sites associated with modulation of frequencies in the 4–12 Hz range (Moran et al., 2010).

Here, we employed a novel EEG network analysis method, Brain Network Activation (BNA) algorithm (Reches et al., 2013; Shahaf et al., 2012), to isolate the characteristic network patterns associated with neural task-based responses modulated by donepezil (for details see "BNA analysis" in Methods). BNA is based on the high temporal resolution of ERPs, and by using a formal graph representation depicts the evolving network dynamics in time, location and frequency. The algorithm explores the time lagged dynamics of the co-occurrence between events, i.e., ERP peaks that belong to different spatial locations and distinct frequency bands. During the search for patterns of network activation composed of time-dependent pairs of events, BNA analysis acknowledges and allows a degree of inter-subject variability and uses an individually-based scoring system in view of the known individual variation in the EEG (Meyer et al., 2013). Hence, the BNA algorithm is congruent with previous studies that identified spatiotemporal patterns of evoked brain electrical activity at different recording sites (Dimitriadis et al., 2012; Gevins and Cutillo, 1993; Gevins et al., 1981; Ioannides et al., 2012; Schinkel et al., 2007) and with the notion that ERPs represent aggregates of underlying neuronal populations (Ba ar, 2004; Bressler, 2002; Fell et al., 2004; Gevins and cutillo, 1993; Skrandies, 2005).

In this study, we focused our analyses on responses to distractors (irrelevant face stimuli) in the context of a visual WM task (Gazzaley et al., 2008) performed by healthy young adults, under placebo and donepezil (single 5 mg dose) treatments using the BNA algorithm. The purpose of this work was to test whether network activation dynamics could serve as a predictive model of the WM performance level. We were particularly interested in characterizing the relationship between individual level of activation of the prefrontal–parietal theta–alpha network and improved performance on the WM task following treatment with donepezil. Our main hypothesis was that the prefrontal–parietal network parameters related to time-dependent events in the theta and alpha frequency bands distributed over different scalp regions will be correlated with WM performance and performance improvement following donepezil.

Methods

Participants

14 healthy paid male and female volunteers, age range 19–30 years participated in the study. All volunteers were right-handed and reported to have normal hearing and normal or corrected-to-normal vision. The protocol was approved by the University of California, Berkeley Institutional Review Board and all participants signed an informed consent before participating in the study.

Study design

This study used the same paradigm and an identical stimulus-set to that reported in Gazzaley et al. (2008). EEG was recorded while participants performed a selective face/scene delayed-recognition task (Fig. 1) to assess WM in the setting of distracting information (Gazzaley et

al., 2008). Participants were given prior knowledge as to which stimulus type was relevant and irrelevant. Each trial contained two faces and two scenes presented sequentially in a randomized order (cue period), each being displayed for 800 ms (200 ms ISI), followed by a 9 s delay period in which the images were to be remembered and mentally rehearsed. After the delay, a third image appeared (Probe) for a duration of 1 s (Fig. 1). The participant was asked to respond with a button press (as quickly as possible without sacrificing accuracy) whether the third image (Probe) matched one of the previous images. Participants were given the following instructions: remember faces (ignore scenes, hereafter, Face Memory), remember scenes (ignore faces, hereafter, Scene Memory) or passively view all stimuli (hereafter, Passive View).

When the probe image appeared, it was composed of a face in the face memory condition, and a scene in the scene memory condition. In Passive View, participants were instructed to relax and view the stimuli without trying to remember them. Instead of a probe image, an arrow was presented and participants were required to make a button press indicating the direction of the arrow (Fig. 1). The task was presented in 3 separate runs (20 trials each) with each of the three conditions in random order. Conditions and stimuli were counterbalanced across participants.

Each participant received either placebo or donepezil (5 mg, orally) on two different visits. Drug administration was double blind, and the order of drug and placebo administration was counterbalanced across participants.

Stimuli

The stimuli consisted of grayscale images of faces and natural scenes. All face and scene images were novel across all conditions and across all runs of the experiment. Images were 225 pixels wide and 300 pixels tall (14×18 cm) and subtended ~5 by 6° of visual angle (participants were ~172 cm from the screen). The face stimuli consisted of a variety of neutral-expression male and female faces across a large age range. The gender of the face stimuli was held constant within each trial, and each stimulus was used in only one trial.

EEG recording and waveform analysis

ERPs were recorded from a 64 channel cap with Ag/AgCl active electrodes (Biosemi Active Two EEG system, Amsterdam, Netherlands) positioned according to the 10–20 international system. Four electrodes, above and below the right eye, and on the outer can thus of each eye served to record eye movements (EOG). Participants were instructed to avoid eye movements, blinking and body movements as much as possible, and to keep their gaze on the center of the screen during task performance. The EEG was sampled at a rate of 256 Hz and stored for off-line analysis. Continuous individual records were subjected to a 0.5–30 Hz band-pass filtering (FIR rectangular filter).

Nuisance components of horizontal eye movements and blinks were removed offline in Matlab (The Mathworks, Natick, MA) using EEGLAB (http://sccn.ucsd.edu/eeglab/index.html) (Delorme and Makeig, 2004). Epochs of EEG from200 to 800 ms post-stimulus onset free of excessive electrical interference (b100 µV) were selectively averaged only for the irrelevant faces stimuli of the Scene Memory condition (Remember Scenes condition).

Thus, in total, 120 epochs were collected per participant (20 trials × 3 blocks × 2 facial stimuli).

ERP measures and electrode selection

The ERPs were time-locked to the onset of the irrelevant faces (from the Scene Memory task). Selection of electrodes for peak identification analysis was a two-stage process. First, several electrodes were selected for each ERP component of interest based on a previous parcellation (Luo et al., 2010) with the addition of the temporo-occipital electrodes, P9/P10, here. Specifically, for the P1 component, electrodes Pz, P3, P4, POz, PO3, and PO4 were selected for statistical analysis (50–150 ms); N170 (120–220 ms) was analyzed at the P7, P8, P9, P10, PO7, and PO8 electrode sites; P3 (300–500 ms) was analyzed at the following 15 electrode sites (FCz, FC3, FC4, Cz, C3, C4, CPz, CP3, CP4, Pz, P3, P4, POz, PO7, and PO8).

Next, electrodes for statistical analyses were chosen by their maximal value at the group level from each of the above clusters (Gazzaley et al., 2008). Thus, each ERP component was finally represented by a single electrode chosen from its corresponding multiple electrode cluster based on its maximum amplitude. Only in the case of the P1 component there was a discrepancy between the maximum-amplitude electrodes of placebo and donepezil, respectively, and the maximum amplitude electrode in the donepezil condition was finally chosen as the representative electrode. For the P1 component PO3 was selected; for N170 electrode, P10 was selected; and for P3 electrode, PO8 was selected.

We conducted repeated measures analyses of variance (ANOVA) with Treatment (donepezil, placebo) and Component (P1, N170, P3) as fixed factors and Participants as a random factor. Using planned contrasts, we compared the amplitude and latency values between treatments for each of the components.

BNA analysis

General principles of the BNA algorithm—BNA is based on identifying patterns of phase-locked evoked activity and it relates network dynamics to several network parameters. Specifically, the Brain Network Activation (BNA) algorithm exploits the inter-participant sequential *temporal* co-occurrence of pairs of ERP peaks (event-pairs) extracted from signals that were band-pass filtered into different *frequency* ranges and that emerged in different *spatial* locations. Thus, BNA captures the dynamic integration of event-pairs of specific temporal relations, spatial locations and frequencies into a unified functional network. Hence, BNA relies on a tridimensional analysis (Stephane et al., 2012) of time-dependent event-pairs across a group of participants. It is noteworthy that BNA describes functional connections which are not based on correlations of oscillatory activity (e.g., Brázdil et al., 2013) but rather on the temporal co-occurring pairs of ERP peaks.

As mentioned above, the information regarding the temporal co-occurring event-pairs which form into patterns is extracted from the participants of the *group*. That is, only if a specific sequential activation pattern of co-occurring ERP peaks is common across participants included in the group it will be considered as the characteristic group's network. Therefore,

the coordinated activity in time, location and frequency depicted in the BNA group's network imply that the spatiotemporal functional dependencies of regional neuronal activities in different frequency bands represent functional links common to and characteristic of a specific population (e.g. healthy controls, Alzheimer disease patients). Individual brain activation patterns are compared against the group's network to determine the degree of similarity between the two in terms of network dynamics. The degree of similarity is measured by the BNA score as detailed in "Single participant level process and the BNA score" below.

The BNA method allows an encompassing description of brain activation using a graph as the formal representation of a network in which the nodes represent events defined in time, location and frequency-band, and the edges represent consistent temporal activity among nodes. This is a suitable and convenient formal representation of the sequence of time-dependent activations that occur in different frequency-bands and scalp-locations. This formal representation allows a comparison between entire networks representing different groups or conditions as well as the comparison of the single participant to the group by comparing between different multidimensional graphs. This approach is in accordance with the view that cognition results from dynamic interactions of distributed brain areas operating in large-scale networks (Bressler and Menon, 2010).

Detailed description of the BNA algorithm: Two main processes—The BNA analysis involves two independent processes (Figs. 2A–H), a group level pattern recognition process (blue arrows, Fig. 2) and a single participant level similarity evaluation process (red arrows, Fig. 2). The group level process does not consist on averaging across participants, which masks variability within the group, but is rather based on identifying the largest common denominator of activation across participants while still preserving the inter-subject variability of individual participants (for more details see sub-section "Group level process" below).

At the group level, patterns are extracted from EEG data recorded from members of a group of participants, all of whom have undergone the same task. In the single participant level process, EEG data from a single participant external to the group, who underwent the same task, is evaluated against a set of extracted group patterns. A BNA score reflecting the degree of congruity between the participant's pattern of activation and that of the group's is assigned for each individual participant. The two processes will now be described in more detail.

Group level process: The first stage in the group level pattern recognition process involves *data preprocessing* (Figs. 2A–C). At this stage continuous individual records undergo initial band-pass pass filtering followed by artifact rejection and band-passing to the conventional EEG frequency bands: delta (0.5–4 Hz), theta (3–8 Hz), alpha (7–13 Hz) and beta (12–30 Hz). All overlapping frequency bands were used in the next steps of the analysis to reduce loss of information. The outcome of this analysis stage is a set of EEG time-domain waveform signals per individual frequency band per electrode location. Next, the continuous filtered data is segmented into epochs, sorted according to stimulus type and

averaged within each separate frequency band to obtain the ERPs. For further details see "EEG recording and waveform analysis" above.

Second, *salient event extraction* is performed (Figs. 2D, E). This stage reduces an individual's continuous ERP record into a set of discrete events (peaks and troughs) representing waveforms in each of the frequency bands defined above. For each participant all the minimal and maximal peaks from all frequency bands and electrodes that surpassed a specific threshold are selected for further analysis as follows. Initially, the average frequency band is calculated based on the high and low boundaries of the given frequency band. Next, the percentage threshold, which is the inverse of the average frequency, is computed per frequency band. Finally, the number of peaks selected for analysis is determined by the percentage threshold of the highest normalized peaks (see Appendix A, "Normalization procedure"). This procedure ensures that signals are adequately represented across frequency bands. The selected peaks are considered salient events, each with a defined latency, amplitude, frequency band and location on the scalp, i.e., in a four dimensional space (Figs. 2D, E).

Following the salient-event waveform extraction stage described above, in the third stage, *network analysis* is performed (Figs. 2F, G). In this stage, BNA identifies functional networks that provide stimulus and task-related structures in the *time–location–frequency* space of the EEG. BNA first locates clusters that include all or most participants in the group. Each cluster represents a single activity (negative or positive ERP peak) common to the group, over a defined location on the scalp, within a narrow frequency band and with narrow latency and amplitude ranges (this cluster will hereafter be referred to as a group common 'unitary event'). Following unitary event extraction, the algorithm seeks time-dependent 'event-pairs', defined as any two salient events (ERP peaks) in a single participant, each of which is included in a separate unitary event at a given scalp location and at a given frequency band and that maintain a specific temporal relation between them. The BNA algorithm extracts spatiotemporal patterns composed of a set of such temporally-dependent event-pairs contained in multiple unitary events. Previously it was shown that volume conduction is unlikely to be responsible for the temporal contingency between events (Shahaf et al., 2012).

Each of the events comprising an event-pair is obeying an absolute temporal constraint on its latency (i.e. the *absolute time* constraint) and both of the events are obeying a relative temporal constraint for the inter-event interval (i.e. the *relative time* constraint) across a group of participants. Specifically, the *absolute time* is the latency of an event locked to stimulus onset, while the *relative time* is the time difference between the latencies of the events comprising the event-pair. The group pattern is then composed of all pairs of temporally co-occurring events that are common to the group from all electrode locations/ frequencies. The term 'temporally co-occurring' refers to a fixed relative time between the two events in each of the participant's event-pairs.

Event-pair identification consists of a sliding adjustable rectangular window which searches for clusters of event-pairs across all participants (Fig. 3). The horizontal side of the rectangle represents the absolute time of events while the vertical side represents the interevent

interval. The plane bounded by the rectangle defines a cluster of event-pairs satisfying both absolute and relative time constraints in order to locate collections of tightly-spaced points with a minimum number of participants determined by a threshold (see Shahaf et al., 2012). This defined collection of event-pairs across individual participants is represented in the group network that preserves inter-subject variability and therefore allows the comparison of the individual activation to the group's pattern.

Single participant level process and the BNA score: The single participant level similarity evaluation process (red arrows) involves three stages of which the first two (data preprocessing and salient event extraction) (Figs. 2A–E) are identical to the first two stages of the group level process. In the third stage, event-pairs from single participants, that did not participate in the group network, are compared to corresponding event-pairs in the group network (Fig. 2H) to assess the degree of similarity between the two. The comparison results in a BNA score with a value ranging between 0 and 100, where 100 designates complete congruence in terms of the network activation pattern between the single participant and the group's pattern that functions as a reference brain network.

More specifically, the BNA score is the measure of the functional similarity between the activation pattern of a single participant and the group's network in terms of the sequence of the temporal co-occurrence of event-pairs. The timing parameters that define co-occurrence are associated with event pairs of specific spatial locations and frequencies and therefore the BNA score reflects the similarity level between the activation pattern of the single participant and the group's network in all three dimensions: time, location and frequency (for the exact calculation of the BNA score see Appendix B, "BNA score computation").

For computing the BNA score, individual activation that was recorded for participants under placebo can be assessed against the reference group network under donepezil and vice versa (that is, the treatments could be swapped between the single-participant level and the group level). This possible incongruence of conditions between the individual and the group level while computing the BNA score is made possible since the extraction of activation patterns is divided into two independent processes: the single participant level and the group level process, respectively. This incongruence between conditions could be evident, for example, when BNA scores obtained for participants treated with placebo are separately computed against each reference (group) network of placebo and donepezil, respectively.

The single participant BNA score could be applied to entire networks as described above or else to sub-networks, that is, portions of the network, hereafter termed sub-BNA (sBNA) analysis. sBNA may be employed to calculate the single participant BNA score relative to a sub-network that is a-priori selected for post-hoc analyses.

Comparing the mean BNA score between networks—To test whether the placebo and/or the donepezil network significantly differentiated between placebo and donepezil treatments, individual network activity scores were first computed. That is, individual BNA scores were calculated by comparing the single participant activity to the placebo and donepezil group characteristic networks. These computations yielded placebo network BNA scores and donepezil network BNA scores, respectively. Placebo network

BNA scores and donepezil network BNA scores were computed separately for each treatment, i.e. once when the participants received placebo and once when they received donepezil, yielding two sets of scores per network.

Then, Wilcoxon signed-rank test was used to test significance of within-group differences in BNA scores obtained in each of the treatments, placebo and donepezil, respectively. Since the computation of a BNA score consists of a comparison between the single participant activity and the group pattern she/he participated in, it is inherently biased due to over-fitting. Therefore, a leave-one-subject-out (LOSO) cross-validation method was used to compute the placebo or donepezil network BNA scores (see further details in Appendix C, "BNA scores: placebo vs. donepezil").

Correlation analyses—To test whether the donepezil network could serve as a model of WM performance, Spearman's rho correlation coefficients were used to examine the relationship between donepezil network BNA score and WN performance. We computed the correlation between performance in the WM task (i.e. accuracy = percent of correct responses) and the donepezil network BNA scores both obtained under placebo. We also tested the ability of BNA to predict beneficial effects of donepezil by calculating the correlation between the donepezil network BNA score for participants under placebo and the difference in WM performance between placebo and donepezil (donepezil minus placebo). Each of the above correlations was re-computed for the theta–alpha sub-network using sub-BNA (sBNA) analysis (see "sBNA post-hoc analyses" below).

sBNA post-hoc analyses—The single participant BNA score could be applied to entire networks as described above or to sub-networks, that is, portions of the network, termed sub-BNA (sBNA) analysis. Thus, we employed sBNA to compute the BNA scores for a sub-network of the donepezil characteristic network (i.e. sBNA scores) that included only theta–alpha connections. This sub-network was chosen based on previous findings in the literature indicating its importance in gating relevant information in the context of WM tasks (as indicated in the Introduction). A prefrontal/occipito-parietal theta–alpha sub-network constituting a unique portion of the donepezil characteristic network was chosen for further analysis using sBNA.

The sBNA was defined based on the literature emphasizing the roles of the frontal and prefrontal regions in top-down control (see a summary in Kawasaki et al., 2010) and on the findings indicating that the functional connections between the frontal theta and posterior alpha regions support working memory (Kawasaki et al., 2010; Moran et al., 2010; Zanto et al., 2011). For extracting the sBNA we chose to focus on frontal and central electrode sites. All possible connections between the frontal/central theta and occipital–parietal alpha nodes were examined. For the frontal and central regions the following electrodes were included: FP1, AF7, AF3, F1, F3, F5, Fpz, Fp2, AF8, AF4, AFz, Fz, F2, F4, F6, FC5, FC3,FC1, C1, C3, C5, CP5, CP3, CP1, CPz, FC6, FC4, FC2, FCz, Cz, C2, C4, C6, CP6, CP4, and CP2. For the occipito-parietal regions the following electrode sites were included: P1, P3, P5, P7, P9, PO7, PO3, POz, Pz, P2, P4, P6, P8, P10, PO8, and PO4. Note that inclusion of electrodes for sBNA analysis was determined on the basis of the relevant regions of interest and not on the basis of the observed specific node activations observed in the donepezil

characteristic network as described in the Results section (Placebo and donepezil characteristic networks).

Results

Behavioral measures

The behavioral data analysis focused on the data collected from the Scene Memory condition in which the faces served as distractors and the scenes as the to-be-remembered items, as guided by the findings of Gazzaley et al. (2008). Both recognition accuracy (hits + correct rejections / total possible items) and response times for the Scene Memory task were compared between treatments (placebo, donepezil) using paired t-tests. Therewere no significant differences in recognition accuracy [placebo = 87.3% (SD = 7.8); donepezil = 89.9% (SD = 6.9] nor in response time [placebo = 1191.6 ms (SD = 387.1); donepezil = 1144.9 ms (SD = 366.0)] between treatments.

ERP analysis

Fig. 4 displays the ERP responses to the irrelevant face stimuli (Scene Memory task) in placebo and donepezil. All neural analyses in this study focus on these stimuli in this condition as guided by the results of the Gazzaley et al. (2008) study, which found that the processing of distractor face stimuli was related to scene memory performance. The stimuli elicited the occipito-temporal P1, which peaked around 125 ms on occipito-temporal (P9/P10) as well as occipital (O1/O2) electrodes and had a frontal negative counterpart over Fz. This component was followed by an occipito-temporal (P9/P10) negative deflection, the N170 (~180 ms), with a positive counterpart frontally (Fz) (also known as vertex positive peak [VPP]). Then, a peak activity around 320–330 ms of a negative slow going deflection proceeded on the central site (Fz), which had a respective positive counterpart over occipito-temporal (P9/P10) and occipital (O1/O2) sites. All of the planned contrasts conducted on the peak amplitude and latency values of each of the components measured at the selected electrodes were not significant. Table 1 displays the average amplitude and latency values of the ERP components.

BNA analyses

Placebo and donepezil characteristic networks—The two most characteristic networks selected by the algorithm as the group networks for the placebo and donepezil treatments elicited by irrelevant face stimuli during the cue period of the "Scene Memory" condition are depicted in Figs. 5A and B, respectively. These images display characteristic network activity overlaid on a scalp electrode montage.

Each of the networks displayed above the corresponding gray column (Figs. 5C and D, respectively) is a superposition of all the separate time points at which specific network activity was present. The evolution over time (in ms) of the placebo (A) and donepezil (B) networks is displayed within the gray columns for each characteristic network, (C) and (D), respectively. Overall, the networks are similar, as both involved connections between central theta activity and posterior parieto-occipital theta. However, the donepezil network also included a more frontal activation and more left-lateralized fronto-central activation relative

to the placebo network. In addition, a dual-frequency pattern emerged in the donepezil network comprising both theta and alpha activations, whereas the placebo network was characterized by only homogeneous theta dynamics.

The major differences between the two treatments can be observed in the ~120–140 ms and ~200–220 ms time intervals, respectively (Figs. 5C and D). These time intervals are those in which theta and alpha activations were more prominent (relative to other time frames) as denoted by the stronger hue of color in those intervals (see legend). In the earlier interval, the right frontal (F2, F4, FC4) and occipital theta (O1, O2, PO8) activation emerged in the donepezil treatment (Fig. 5D) while it was absent in the placebo network (Fig. 5C). In the later time interval, theta activation was more prominent fronto-centrally on the left side in the donepezil treatment, while it was scarcer in the placebo treatment and appeared on the right side. It is noteworthy that at 120 ms, a bi-spectral pattern emerged in donepezil including both theta and alpha unitary events occurring intra-regionally in frontal (F2) as well as in occipital sites (O1, O2, PO8) (Fig. 5B).

A Wilcoxon signed-rank test comparison of the individual BNA scores (mean ± SD) between placebo (39.6 ± 23.3) and donepezil (55.4 ± 25.7) treatments revealed a significant difference only for the donepezil network (p b 0.05). Since the BNA score reflects the degree of similarity between the individual event-pairs and the corresponding event-pairs in the group network (see Methods), this finding means that significant elements of the donepezil group-level network could not be consistently found in the activations of individual placebo participants (i.e. the theta–alpha coupling between fronto-central and posterior regions, Fig. 5). This suggests that the extra bi-spectral coupling in the donepezil network at ~120–140 ms after the irrelevant face stimulus is reflective of distractor processing that is present following donepezil treatment and is absent following placebo.

Correlation analyses between BNA scores and performance accuracy—To first test whether the donepezil network could serve as a predictive model of WM performance, we calculated Spearman's rank correlation between accuracy, as measured in the Scene Memory condition, and individual BNA scores. For this analysis, the donepezil network BNA scores for participants under placebo were calculated. The correlation with accuracy scores turned out to be positive and significant ($r_s = 0.62$, $p < 0.05$) (Fig. 6A). Fig. 6A shows that participants who received a higher BNA score in the placebo condition, i.e., those participants with a higher level of similarity to the donepezil network in placebo, were better performers on the WM task in the placebo condition.

To test the donepezil network as a predictive model of beneficial drug effects, an across-participant Spearman's rank correlation was calculated between the donepezil network BNA scores of participants in the placebo condition and the accuracy difference between placebo and donepezil. This correlation was found to be negative and insignificant ($r_s = -0.47$, $p = 0.09$).

Correlation analyses between sBNA scores and performance accuracy—A fronto/central–parietal theta–alpha sub-network constituting a unique portion of the donepezil characteristic network (Fig. 5B) was chosen for further analysis using sBNA (Fig.

6B). We re-computed the two correlation analyses carried out with the donepezil network BNA scores (see "Correlation analyses" above) with the theta–alpha sub-network sBNA scores (see Methods). The donepezil sub-network sBNA scores of participants in the placebo condition yielded significant Spearman's rank correlations with performance accuracy (r_s = 0.55, $p < 0.05$) (not shown) and with performance accuracy difference scores between placebo and donepezil (r_s = −0.74, $p = 0.01$) (Fig. 6C). Note that the transition from BNA to sBNA scores improved the correlation with performance accuracy difference and in contrast to the former resulted in a significant correlation. Fig. 6C demonstrates that the further away a participant is from the donepezil characteristic network when under placebo, i.e., those participants with a lower level of similarity to the donepezil network, the greater their performance improvement on the WM task following donepezil treatment (hereafter will be referred as 'responders'). Importantly, the correlation also demonstrates that most of the participants that received a higher sBNA score (upper left side of the graph), i.e., those with a higher level of similarity to the donepezil network in placebo, exhibited a deterioration of performance following donepezil administration (hereafter will be referred as 'non-responders').

Discussion

Summary of main findings

In the current study, we examined the effects of cholinergic manipulation using donepezil on the relationship between WM performance and network dynamics during distractor processing across individuals. BNA, a novel method of neural network extraction based on ERPs (Shahaf et al., 2012), revealed that while the donepezil network significantly differentiated between the BNA scores of individuals undergoing placebo and donepezil treatments the placebo network failed to do so. This means that there were unique elements of the donepezil network consistently found among donepezil participants that could not be found in the activations of individual participants under the placebo condition (i.e. fronto-central theta and posterior alpha coupling, Fig. 5), but not the reverse scenario.

Results further indicated that those participants with a higher donepezil network BNA score under placebo performed better on the WM task in the placebo condition. That is, the more similar the basal activation of an individual is to the donepezil network the better the WM performance. In other words, the individual level of similarity to the donepezil network, as reflected by the BNA score, serves as a predictor of WM performance.

Moreover, those participants with a *lower* basal level of similarity to the sBNA donepezil network (Fig. 6B) benefited the most from donepezil administration as measured by the change in WM performance following donepezil administration. That is, participants with a lower basal congruence to the sBNA donepezil network under placebo showed greater improvement in WM task performance following donepezil administration. The strong correlation of the theta–alpha sBNA network with the magnitude of performance improvement following donepezil underlies the crucial element in the donepezil network functional dynamics, namely, the joint activation of frontal theta and posterior alpha. Overall, these results support the hypothesis of the study and indicate that the donepezil

network might serve as a model of WM performance, emphasizing the possible role of the cholinergic system in top-down modulation of visual features.

The theta–alpha sBNA network

The fact that during face distractor processing the level of similarity to the fronto/central–parietal theta–alpha sBNA network (Fig. 6B) was correlated with the magnitude of scene WM accuracy improvement following donepezil treatment (Fig. 6C) highlights the importance of this network for representing and maintaining relevant information (Fuster et al., 1985; Gazzaley et al., 2004; Knight et al., 1999; Moran and Desimone, 1985; Rainer et al., 1998; Rissman et al., 2004; Rutman et al., 2010; Shimamura, 1997; Zanto and Gazzaley, 2009; Zanto et al., 2011). These results are in line with previous findings suggesting that theta and alpha oscillations interact at modality-specific posterior regions, while theta synchronizations connect fronto-central and posterior regions for manipulation of stored representations (Kawasaki et al., 2010).

Our results showed that theta–alpha simultaneous activation over posterior sites occurs at early stages of visual processing (~120 ms). The P1 component also occurs during this time frame, and has been previously shown to serve as a neural marker of top-down modulation for visual features and objects (Gazzaley et al., 2008; Rutman et al., 2010; Zanto and Gazzaley, 2009; Zanto et al., 2010, 2011). Since the P2 component reflects the matching process between sensory inputs and stored representations (Freunberger et al., 2007; Luck and Hillyard, 1994) it could be that the more prominent theta activation at ~200 ms indicates theta involvement in inhibiting irrelevant information in accordance with the suggestion that frontal theta activity is linked to central executive functions (Kawasaki et al., 2010). The prominent dominance of theta networks identified in our study is in line with the view that theta oscillations are important for the control of working memory functions (Cohen and Ridderinkhof, 2013; Onton et al., 2005; Sauseng et al., 2009).

The theta–alpha sBNA network accentuated the difference between participants showing improvement ("responders") and deficits ("non-responders") in task performance following donepezil treatment. Specifically, participants with a lower level of similarity to the pre-drug sBNA donepezil network benefited from donepezil administration while participants that received a higher sBNA similarity score under placebo either did not improve or received a negative difference performance accuracy score (indicating impaired performance following donepezil) (Fig. 6C). These results support the possibility that long-range functional connections between fronto/central theta and parietal alpha activations attenuate the influence of distractors during the processing of relevant stimuli and that these specific connections were strengthened following donepezil in pre-treatment low sBNA score individuals. Interestingly, it was also previously found that the theta–alpha frequency range can distinguish between high and low WM capacity individuals (Moran et al., 2010).

In addition, previous findings indicate that theta oscillations are important for the control of working memory functions (Cohen and Ridderinkhof, 2013; Onton et al., 2005; Sauseng et al., 2009) and that alpha is implicated in goal-directed inhibition of task-irrelevant information and sensory-gating of visual inputs over the posterior cortex (Jensen et al., 2012; Mathewson et al., 2011). Taken together, the results of this study support the suggestion that

the functional link between the frontal theta and posterior alpha reflects frontal midline theta activity monitoring or controlling inhibitory posterior alpha activity (Broussard, 2012; Cohen and Ridderinkhof, 2013; Kawasaki et al., 2010; Min and Park, 2010; Payne and Kounios, 2009).

Donepezil might induce an inverted U-shape relationship between BNA score and performance

The correlation between the sBNA scores associated with the theta–alpha network and the change in performance between pre- and post-donepezil administration may be the consequence of an inverted U-shaped relationship that exists between the level of similarity to this network and performance. Specifically, individuals with a higher level of pre-drug similarity to the theta–alpha donepezil sub-network (those with a higher sBNA score in placebo) either did not improve or deteriorated in performance level following donepezil while those with a lower level of pre-drug similarity to the donepezil sub-network benefited more from donepezil administration (see Cools et al., 2009; Husain and Mehta, 2011). Thus, an inverted U-shaped relationship may be exemplified by the relationship between the donepezil network score and performance, specifically the descending portion of the curve.

Previous findings support a U-shaped relationship between donepezil and performance. Donepezil has been previously shown to reduce the decline of visual short-term memory and verbal episodic memory in healthy individuals, mainly in those individuals vulnerable to cognitive impairment following sleep deprivation. On the other hand, in the visual short-term memory task the performance of participants who were not as affected by sleep deprivation tended to deteriorate after donepezil intake (Chuah and Chee, 2008; Chuah et al., 2009). These results demonstrate the relationship between the pre-medicated level of cognitive function and the effect of medication on performance that might fit such a U-shaped function as described above.

Donepezil increases cholinergic synaptic transmission in the brain by reducing the activity of the enzyme that breaks down ACh. While this study has not offered direct evidence for a correlation between proximity to the donepezil pattern and ACh levels it is possible that the possible inverted U-shaped relationship between the BNA score and cognitive performance is at least partially mediated by ACh. In line with this suggestion, in this study, high-synthesis ACh participants might actually be impaired in their performance following the administration of donepezil (non-responders), while those with low neurotransmitter level and accompanying low baseline working-memory spans might benefit more from drug administration (responders) (see Husain and Mehta, 2011).

Similarly, the large variability in response improvement among neurologic patient groups following treatment with AChEIs may be explained by baseline indicators of network function (Husain and Mehta, 2011). Of note, U-shaped like effects have been well characterized for the dopamine system in studies involving experimental animals that show inverted U-shaped relationship between dopamine receptor levels and cognitive performance (Vijayraghavan et al., 2007; Williams and Goldman-Rakic, 1995; Zahrt et al., 1997).

The inverted U-shaped relationship demonstrated in this study could also be responsible for the lack of significant overall difference in performance measures between treatments. Since the entire group of participants was heterogeneous in terms of response improvement there was a large variability of response, with some participants showing no improvement or impaired performance (non-responders) and others showing strong improvement. Thus, the drug effect was offset since many individuals showed little benefit and even deterioration in cognitive performance following donepezil (see Husain and Mehta, 2011).

It should be emphasized, however, that the correlation between the sBNA scores associated with the theta–alpha network and the change in performance between pre- and post-donepezil administration may be the consequence of regression to the mean, i.e., those individuals with better WM performance in placebo deteriorated with donepezil and those with worse WM performance in placebo improved with donepezil. Thus, in the current dataset, we cannot rule out the possibility that the hypothesized inverted U-shaped pattern described above between sBNA scores and performance improvement is at least in part driven by the regression to the mean effect. This will be explored in future studies.

Methodological issues

BNA in view of other network analysis methods—Existing methods of network analysis are based on different types of interdependencies such as temporal correlations (Rubinov and Sporns, 2010; Stam, 2005; Stam et al., 2007; Zhou et al., 2009), coherence across brain regions (Murias et al., 2007; Salvador et al., 2005; Sun et al., 2004; Zhou et al., 2009) and synchronization likelihood between electrodes (Ahmadlou and Adeli, 2010). Other approaches to characterize large-scale networks (Bullmore and Sporns, 2009; Rubinov and Sporns, 2011; Stam et al., 2007) use different aspects of graph theoretical analyses (De Vico Fallani et al., 2008) including small world networks (Bassett and Bullmore, 2006), multiscale data mining (Eldawlatly et al., 2009), and interdependencies between and within community structures (Ahmadlou and Adeli, 2011).

A common denominator across most of these methods is that individual measures based on bivariate or multivariate synchronizations are used to characterize patterns of functional integration and segregation within and between brain regions or community structures. Moreover, the vast majority of existing methods that characterize structural or functional networks have been based on properties of static graphs where the links between brain regions (nodes) remain static over time in the sense that the associations between nodes are estimated based on either long or stringent time-windows, whereas brain networks exhibit rapid dynamic changes (Dimitriadis et al., 2010, 2012).

In contrast, the BNA algorithm enables to track dynamic network organization in high temporal resolution using a three dimensional formal graph representation system that depicts the evolution of event pairs in different spatial locations and frequency bands. Hence, the focus of BNA is not on discrete parameters of EEG activity (such as spectral power) but on the entire network configuration which is compared between different groups and conditions.

BNA and its relation to ERP generation models—In the existing literature, two main models explain the generation of an ERP component, phase synchronization, also known as phase-resetting or phase-alignment and additive neural activity (see a review in David et al., 2005 and in Mishra et al., 2012). According to the first explanation, ongoing oscillatory activity produces an ERP without changes in the amount of activated neurons, while according to the latter option ERPs stem from event-related activation distinct from ongoing background dynamics (Fell et al., 2004).

BNA methodology is related to a recently suggested model that explains event-related changes in the EEG, the 'Firefly model' (Burgess, 2012). The Firefly model belongs within the phase-alignment family of theories. According to this model, phase synchronization is achieved by frequency adjustment among neuronal networks with the same preferred frequency of oscillation and it is this coordination across the frequency range that generates the ERP. In the 'Firefly model' study the EEG was decomposed into components comparable to harmonic functions in FFT. Most of these components had a time-varying frequency in the delta, theta and alpha frequency ranges, which correspond to the frequency bands that are functionally related to a meaningful cognitive processing (e.g. Klimesch et al., 1999). Since we have used single-trial filtration to extract the frequency bands of different peaks, each discrete ERP peak represents a waveform of the original signal of specific wavelength congruent with the specific band-pass used for filtration. If it can be assumed that the emergence of ERPs can be at least partially accounted for by phase resetting of EEG oscillations, then the co-occurring pair of ERP peaks from two different frequencies (or from the same frequency) in the BNA network may represent a temporal contingency between two different oscillations. Nevertheless, it should be noted that the phase-locking to the external stimulus at each electrode could look like inter-electrode coherence (Srinivasan, 2004). Therefore, it may be that a third variable is causing the correlation to occur.

It is noteworthy that the averaged scalp recorded ERPs are not fully represented by EEG oscillatory activity (Müller and Anokhin, 2012). Therefore, it must be stressed that BNA is not directly based on the analysis of EEG oscillations. Hence, it is important to emphasize that the terms used throughout this paper to describe BNA activation as "theta–alpha sub-network" or "theta–alpha connections" relate to peaks of waveforms of specific wavelengths which are congruent with the specific band-pass used for filtration. Thus, the reader should keep in mind that the apparent homology between our findings and studies of oscillatory activity that are cited throughout this paper (Broussard, 2012; Kawasaki et al., 2010; Payne and Kounios, 2009) were achieved while using different methodologies.

Regardless of the mechanism that underlies ERP generation (Makeig et al., 2002; Sauseng and Klimesch, 2008) event-related potentials convey important information regarding early cognitive processing (Mishra et al., 2012; see also Sauseng and Klimesch, 2008) and cognitive functions such as attentional selection mediated by top-down control (Slagter et al., 2005). The goal of BNA analysis is identifying dynamic activation patterns based on ERP peaks that depict cognitive processes immediately ensuing stimulus processing in the context of task performance. Thus, the BNA algorithm is in line with the importance of exploring extrinsic (task-based) functional networks as revealed by functional magnetic

resonance imaging (fMRI) (Mennes et al., 2013) as well as by electrophysiology (Luczak et al., 2009).

Conclusions

Overall the results of this study indicate that the donepezil characteristic network could serve as a model of WM performance and support previous findings showing that cholinergic modulation increases neural selectivity for incoming information (Freo et al., 2005; Hasselmo, 2006; Kukolja et al., 2009; Pa et al., 2013). The findings also support the suggestion that AChEI administration needs to be selective and tailored to each individual (Balsters et al., 2011; Rogers et al., 1998). The theta–alpha sBNA network was found to be sensitive in diagnosing those individuals whose performance would be impaired by the drug. This result might indicate that donepezil specifically impacts theta–alpha connections that are also responsible for the individual differences observed in the level of WM performance.

Following further validation with different populations (e.g. healthy older adults participants, MCI and AD patients) the sBNA theta–alpha network could potentially serve as a predictive model aiding in diagnosing those individuals who may benefit from donepezil as a cognitive enhancer. The findings of this study also indicate that the BNA methodology might contribute to the identification of the mechanism of action underpinning improvement on cognitive tasks following pharmacological administration. The relationships between the results obtained by BNA and other methods relying on non-phase-locked responses should be further examined in future studies.

Appendix A. Normalization procedure

The normalization process was carried out separately for each participant. All minimal and maximal peaks were extracted from the ERPs, for each frequency band and for each electrode. Next, the amplitude of the peaks of each frequency band and electrode was z-score normalized using the standard deviation of the corresponding ERP waveform. Finally, *all* electrodes were pooled together within each frequency band and the highest normalized peaks were selected in the following manner. In the first step, the average frequency band was calculated based on the high and low boundaries of the frequency band:

$$\text{Average} \quad \text{frequency} = \frac{\text{high}_{\text{frequency}} + \text{low}_{\text{frequency}}}{2}. \quad \text{(A.1)}$$

In the second step, the percentage threshold was computed per frequency band as follows:

$$\text{Percentage} \quad \text{threshold} = \frac{1}{\text{Average} \quad \text{frequency}} \times 100. \quad \text{(A.2)}$$

The number of peaks selected for analysis was determined by the percentage threshold of the highest normalized peaks which were defined as salient events. The percentage of selected peaks using the above formulas is higher for the lower frequencies and lower for the

higher ones. This procedure ensured that signals were adequately represented across frequency bands.

Appendix B. BNA score computation

Previously (Shahaf et al., 2012), the BNA score was computed by assigning a similarity index (SI) of 1 if the activity of the participant included the same event-pairs as in the group level or otherwise a score of 0. In the former case, the SI was multiplied by the weight of the connection between two evens within the event-pair (see Shahaf et al., 2012). The weight is based on the number of participants sharing the pair, and the variability of the absolute and relative times of the pair across participants. However, in the current study we used a Gaussian probability distribution function (PDF) to calculate the SI, which was then multiplied by the weight of each event-pair in the pattern. We will now detail the steps that lead to the calculation of the BNA score.

First, each pair of events in the group's network was searched in the activation pattern of the single participant. An event-pair was scored only if each of the events in the pair resided at the same electrode location and frequency band as the corresponding events at the group level. If this congruence in location and frequency occurred, the absolute and relative times of each of the event-pairs of the single participant were scored relative to the distribution of the corresponding parameters at the group level (Eqs. (B.1) and (B.2)). The *absolute time* is the latency of an event locked to stimulus onset, while the *relative time* is the time difference between the latencies of the events comprising the event-pair. The SI was then obtained by averaging the absolute BNA score and the relative time BNA score (Eq. (B.3)).

To calculate the absolute time(absTime), the participant's timings of a pair of events are compared each to the distribution of the group's corresponding timings of these events. The scores for each of the events are then averaged, as follows:

$$\text{absTime}_i = \frac{\text{Normal}(t1_i, [\text{mean}(T1_i), \text{std}(T1_i)]) + \text{Normal}(t2_i, [\text{mean}(T2_i), \text{std}(T2_i)])}{2} \quad \text{(B.}$$

1)

where:

$Normal(x, [mean, std])$ denotes a normal distribution.	
i	is an index of one of the pattern's event-pairs.
$T1_i, T2_i$	are the latencies of the first and second event of the event-pair (group level).
$t1_i, t2_i$	are the timings of the closest event-pair of the single participant to the means of $T1_i$ and $T2_i$ respectively.

To calculate the relative time (*relTime*), the difference between the latencies of the two events in an event-pair of the single participant was calculated and then compared to the distribution of the difference of this exact event-pair at the group level, as follows:

$$\text{relTime}_i = \text{Normal}(\text{abs}(t1_i - t2_i), [\text{mean}(T2_i - T1_i), \text{std}(T2_i - T1_i)]). \quad \text{(B.2)}$$

The SI was then computed by averaging the absolute time(Eq. (B.1)) and the relative time (Eq. (B.2)):

$$\text{SI}_i = (\text{absTime}_i + \text{relTime}_i)/2. \quad \text{(B.3)}$$

In the next step, the calculation of the weight of each of the event-pairs in the pattern was performed as follows:

$$W_i = \frac{n_i}{n_p} \times \frac{\max(Tstd) - \max(std(T1_i), std(T2_i))}{2 \times \max(Tstd)} \times \frac{\max(Trel\_std) - std(Trel_i)}{2 \times \max(Trel\_std)} \quad \text{(B.4)}$$

where:

n_i	is the number of participants sharing the event-pair.
n_p	is the number of participants sharing the entire pattern.
Tstd	is a vector of all the stds of the absolute timings of the event-pairs in the pattern.
Trel_std	is a vector of all the stds of the relative timings of each of the event-pairs in the pattern.

Finally, the *BNA score* of a single participant was then calculated by computing the weighted average of all the SI scores of each of the single participant's event-pairs in the pattern.

$$\text{BNA score} = \frac{\sum_{i=0}^{N}(W_i \times SI_i)}{\sum_{i=0}^{N} W}. \quad \text{(B.5)}$$

Appendix C. BNA scores: placebo vs. donepezil

To test whether there was a significant difference of the BNA score between the two treatments per a specific network (placebo/donepezil) a BNA combined score was computed as follows. For each participant, the BNA score was computed twice relative to a network representing a specific treatment, e.g. placebo: 1) when the participant participated in the placebo treatment, and 2)when the same participant participated in the donepezil treatment. Finally, a two-tailed paired *t*-test was performed comparing the means of the two sets of BNA scores per specific network (placebo, donepezil). The same procedure was applied on the donepezil network. To compute the BNA score relative to each of the placebo and

donepezil networks, respectively, a Leave-One-Subject-Out (LOSO) cross-validation method was employed. Each participant in turn was left out of her/his own core group (e.g. placebo) and the BNA score was then computed for each participant against the most representative group pattern (excluding the tested participant).

References

Ahmadlou M, Adeli H. Wavelet-synchronization methodology: a new approach for EEG-based Diagnosis of ADHD. Clin. EEG Neurosci. 2010; 41:1–10. [PubMed: 20307009]

Ahmadlou M, Adeli H. Functional community analysis of brain: a new approach for EEG-based investigation of the brain pathology. Neuroimage. 2011; 58:401–408. [PubMed: 21586331]

Balsters JH, O'Connell RG, Martin MP, Galli A, Cassidy SM, Kilcullen SM, Delmonte S, Brennan S, Meaney JF, Fagan AJ, Bokde AL, Upton N, Lai R, Laruelle M, Lawlor B, Robertson IH. Donepezil impairsmemory in healthy older subjects: behavioural, EEG and simultaneous EEG/fMRI biomarkers. PLoS One. 2011; 6:e24126. [PubMed: 21931653]

Ba ar E. Macrodynamics of electrical activity in the whole brain. Int. J. Bifurc. Chaos. 2004; 14:363–381.

Bassett DS, Bullmore E. Small-world brain networks. Neuroscientist. 2006; 12:512–523. [PubMed: 17079517]

Bastiaansen MC, Posthuma D, Groot PF, deGeus EJ. Event-related alpha and theta responses in a visuo-spatial working memory task. Clin. Neurophysiol. 2002; 113:1882–1893. [PubMed: 12464325]

Birks J. Cholinesterase inhibitors for Alzheimer's disease. Cochrane Database Syst. Rev. 2006; 25:CD005593. [PubMed: 16437532]

Brázdil M, Jane ek J, Klimeš P, Mare ek R, Roman R, Jurák P, Chládek J, Daniel P, Rektor I, Halámek J, Plešinger F, Jirsa V. On the time course of synchronization patterns of neuronal discharges in the human brain during cognitive tasks. PLoS One. 2013; 8:e63293. [PubMed: 23696809]

Bressler, SL. Event-related potentials. In: Arbib, MA., editor. The Handbook of Brain Theory and Neural Networks. Cambridge MA: MIT Press; 2002. p. 412-415.

Bressler SL, Menon V. Large-scale brain networks in cognition: emerging methods and principles. Trends Cogn. Sci. 2010; 14:277–290. [PubMed: 20493761]

Broussard JI. Posterior parietal cortex dynamically ranks topographic signals via cholinergic influence. Front. Integr. Neurosci. 2012; 6:32. [PubMed: 22712008]

Bullmore E, Sporns O. Complex brain networks: graph theoretical analysis of structural and functional systems. Nat. Rev. Neurosci. 2009; 10:186–198. [PubMed: 19190637]

Burgess AP. Towards a unified understanding of event-related changes in the EEG: the firefly model of synchronization through cross-frequency phase modulation. PLoS One. 2012; 7:e45630. [PubMed: 23049827]

Chadick JZ, Gazzaley A. Differential coupling of visual cortex with default or frontal–parietal network based on goals. Nat. Neurosci. 2011; 14:830–832. [PubMed: 21623362]

Chuah LY, Chee MW. Cholinergic augmentation modulates visual task performance in sleep-deprived young adults. J. Neurosci. 2008; 28:11369–11377. [PubMed: 18971479]

Chuah LY, Chong DL, Chen AK, Rekshan WR III, Tan JC, Zheng H, Chee MW. Donepezil improves episodic memory in young individuals vulnerable to the effects of sleep deprivation. Sleep. 2009; 32:999–1010. [PubMed: 19725251]

Cohen MX, Ridderinkhof KR. EEG source reconstruction reveals frontal–parietal dynamics of spatial conflict processing. PLoS One. 2013; 8:e57293. [PubMed: 23451201]

Cools R, Frank MJ, Gibbs SE, Miyakawa A, Jagust W, D'Esposito M. Striatal dopamine predicts outcome-specific reversal learning and its sensitivity to dopaminergic drug administration. J. Neurosci. 2009; 29:1538–1543. [PubMed: 19193900]

David O, Harrison L, Friston KJ. Modelling event-related responses in the brain. Neuroimage. 2005; 25:756–770. [PubMed: 15808977]

De Vico Fallani F, Astolfi L, Cincotti F, Mattia D, Tocci A, Salinari S, Marciani MG, Witte H, Colosimo A, Babiloni F. Brain network analysis from high-resolution EEG recordings by the application of theoretical graph indexes. IEEE Trans. Neural Syst. Rehabil. Eng. 2008; 16:442–452. [PubMed: 18990648]

Delorme A, Makeig S. EEGLAB: an open source toolbox for analysis of single-trial EEG dynamics including independent component analysis. J Neurosci. Methods. 2004; 134:9–21. [PubMed: 15102499]

Dimitriadis SI, Laskaris NA, Tsirka V, Vourkas M, Micheloyannis S, Fotopoulos S. Tracking brain dynamics via time-dependent network analysis. J. Neurosci. Methods. 2010; 193:145–155. [PubMed: 20817039]

Dimitriadis SI, Laskaris NA, Tzelepi A, Economou G. Analyzing functional brain connectivity by means of commute times: a new approach and its application to track event-related dynamics. IEEE Trans. Biomed. Eng. 2012; 59:1302–1309. [PubMed: 22318476]

Eldawlatly S, Jin R, Oweiss KG. Identifying functional connectivity in large-scale neural ensemble recordings: a multiscale data mining approach. Neural Comput. 2009; 21:450–477. [PubMed: 19431266]

Fell J, Axmacher N. The role of phase synchronization in memory processes. Nat. Rev. Neurosci. 2011; 12:105–118. [PubMed: 21248789]

Fell J, Dietl T, Grunwald T, Kurthen M, Klaver P, Trautner P, Schaller C, Elger CE, Fernández G. Neural bases of cognitive ERPs: more than phase reset. J. Cogn. Neurosci. 2004; 16:1595–1604. [PubMed: 15601521]

Freo U, Ricciardi E, Pietrini P, Schapiro MB, Rapoport SI, Furey ML. Pharmacological modulation of prefrontal cortical activity during a working memory task in young and older humans: a PET study with physostigmine. Am. J. Psychiatry. 2005; 162:2061–2070. [PubMed: 16263845]

Freunberger R, Klimesch W, Doppelmayr M, Holler Y. Visual P2 component is related to theta phase-locking. Neurosci. Lett. 2007; 426:181–186. [PubMed: 17904744]

Fuster JM, Bauer RH, Jervey JP. Functional interactions between inferotemporal and prefrontal cortex in a cognitive task. Brain Res. 1985; 330:299–307. [PubMed: 3986545]

Gazzaley A, Rissman J, Desposito M. Functional connectivity during working memory maintenance. Cogn. Affect. Behav. Neurosci. 2004; 4:580–599. [PubMed: 15849899]

Gazzaley A, Cooney JW, McEvoy K, Knight RT, D'Esposito M. Top-down enhancement and suppression of the magnitude and speed of neural activity. J. Cogn. Neurosci. 2005; 17:507–517. [PubMed: 15814009]

Gazzaley A, Clapp W, Kelley J, McEvoy K, Knight RT, D'Esposito M. Age-related top-down suppression deficit in the early stages of cortical visual memory processing. PNAS. 2008; 105:13122–13126. [PubMed: 18765818]

Gevins A, Cutillo B. Spatiotemporal dynamics of component processes in human working memory. Electroencephalogr. Clin. Neurophysiol. 1993; 87:128–143.

Gevins AS, Doyle JC, Cutillo BA, Schaffer RE, Tannehill RS, Ghannam JH, Gilcrease VA, Yeager CL. Electrical potentials in human brain during cognition: New method reveals dynamic patterns of correlation. Science. 1981; 213:918–922. [PubMed: 7256287]

Hamker FH. The reentry hypothesis: the putative interaction of the frontal eye field, ventrolateral prefrontal cortex, and areas V4, IT for attention and eye movement. Cereb. Cortex. 2005; 15:431–447. [PubMed: 15749987]

Hasselmo ME. The role of acetylcholine in learning and memory. Curr. Opin. Neurobiol. 2006; 16:710–715. [PubMed: 17011181]

Husain M, Mehta MA. Cognitive enhancement by drugs in health and disease. Trends Cogn. Sci. 2011; 15:28–36. [PubMed: 21146447]

Ioannides AA, Dimitriadis SI, Saridis GA, Voultsidou M, Poghosyan V, Liu L, Laskaris NA. Source space analysis of event-related dynamic reorganization of brain networks. Comput. Math. Methods Med. 2012; 2012:452503. [PubMed: 23097678]

Jensen O, Bonnefond M, VanRullen R. An oscillatory mechanism for prioritizing salient unattended stimuli. Trends Cogn. Sci. 2012; 16:200–206. [PubMed: 22436764]

Kawasaki M, Kitajo K, Yamaguchi Y. Dynamic links between theta executive functions and alpha storage buffers in auditory and visual working memory. Eur. J. Neurosci. 2010; 31:1683–1689. [PubMed: 20525081]

Klimesch W, Doppelmayr M, Schwaiger J, Auinger P, Winkler TH. 'Paradoxical' alpha synchronization in a memory task. Cogn. Brain Res. 1999; 7:493–501.

Knight RT, Staines WR, Swick D, Chao LL. Prefrontal cortex regulates inhibition and excitation in distributed neural networks. Acta Psychol. (Amst.). 1999; 101:159–178. [PubMed: 10344184]

Kosovicheva AA, Sheremata SL, Rokem A, Landau AN, Silver MA. Cholinergic enhancement reduces orientation-specific surround suppression but not visual crowding. Front. Behav. Neurosci. 2012; 6:61. [PubMed: 23049505]

Kukolja J, Thiel CM, Fink GR. Cholinergic stimulation enhances neural activity associated with encoding but reduces neural activity associated with retrieval in humans. J. Neurosci. 2009; 29:8119–8128. [PubMed: 19553452]

Labrenz F, Themann M, Wascher E, Beste C, Pfleiderer B. Neural correlates of individual performance differences in resolving perceptual conflict. PLoS ONE. 2012; 7:e42849. [PubMed: 22916169]

Luck S, Hillyard SA. Electrophysiological correlates of feature analysis during visual search. Psychophysiology. 1994; 31:291–308. [PubMed: 8008793]

Luczak A, Barthó P, Harris KD. Spontaneous events outline the realm of possible sensory responses in neocortical populations. Neuron. 2009; 62:413–425. [PubMed: 19447096]

Luo W, Feng W, He W, Wang NY, Luo YJ. Three stages of facial expression processing: ERP study with rapid serial visual presentation. Neuroimage. 2010; 49:1857–1867. [PubMed: 19770052]

Makeig S, Westerfield M, Jung TP, Enghoff S, Townsend J, Courchesne E, Sejnowski TJ. Dynamic brain sources of visual evoked responses. Science. 2002; 295:690–694. [PubMed: 11809976]

Mathewson KE, Lleras A, Beck DM, Fabiani M, Ro T, Gratton G. Pulsed out of awareness: EEG alpha oscillations represent a pulsed-inhibition of ongoing cortical processing. Front. Psychol. 2011; 2:99. [PubMed: 21779257]

Mennes M, Kelly C, Colcombe S, Castellanos FX, Milham MP. The extrinsic and intrinsic functional architectures of the human brain are not equivalent. Cereb. Cortex. 2013; 23:223–229. [PubMed: 22298730]

Meyer MC, van Oort ES, Barth M. Electrophysiological correlation patterns of resting state networks in single subjects: a combined EEG–fMRI study. Brain Topogr. 2013; 26:98–109. [PubMed: 22752947]

Min BK, Park HJ. Task-related modulation of anterior theta and posterior alpha EEG reflects top-down preparation. BMC Neurosci. 2010; 28(11):79. [PubMed: 20584297]

Mishra J, Martínez A, Schroeder CE, Hillyard SA. Spatial attention boosts short-latency neural responses in human visual cortex. Neuroimage. 2012; 59:1968–1978. [PubMed: 21983181]

Montijn JS, Klink PC, van Wezel RJ. Divisive normalization and neuronal oscillations in a single hierarchical framework of selective visual attention. Front. Neural Circ. 2012; 6:22.

Moran J, Desimone R. Selective attention gates visual processing in the extrastriate cortex. Science. 1985; 229:782–784. [PubMed: 4023713]

Moran RJ, Campo P, Maestu F, Reilly RB, Dolan RJ, Strange BA. Peak frequency in the theta and alpha bands correlates with human working memory capacity. Front. Hum. Neurosci. 2010; 4:200. [PubMed: 21206531]

Müller V, Anokhin AP. Neural synchrony during response production and inhibition. PLoS One. 2012; 7:e38931. [PubMed: 22745691]

Murias M, Webb SJ, Greenson J, Dawson G. Resting state cortical connectivity reflected in EEG coherence in individuals with autism. Biol. Psychiatry. 2007; 62:270–273. [PubMed: 17336944]

Onton J, Delorme A, Makeig S. Frontal midline EEG dynamics during working memory. Neuroimage. 2005; 15(27):341–356. [PubMed: 15927487]

Pa J, Berry AS, Compagnone M, Boccanfuso J, Greenhouse I, Rubens MT, Johnson JK, Gazzaley A. Cholinergic enhancement of functional networks in older adults with MCI. Ann. Neurol. 2013; 73:762–773. [PubMed: 23447373]

Palmer AM. Pharmacotherapy for Alzheimer's disease: progress and prospects. Trends Pharmacol. Sci. 2002; 23:426–433. [PubMed: 12237155]

Payne L, Kounios J. Coherent oscillatory networks supporting short-term memory retention. Brain Res. 2009; 1247:126–132. [PubMed: 18976639]

Rainer G, Asaad WF, Miller EK. Selective representation of relevant information by neurons in the primate prefrontal cortex. Nature. 1998; 393:577–579. [PubMed: 9634233]

Reches A, Kerem D, Gal N, Laufer I, Shani-Hershkovitch R, Dickman D, Geva AB. A novel ERP pattern analysis method for revealing invariant reference brain network models. Funct. Neurol Rehabil. Ergon. 2013; 3:295–317.

Rissman J, Gazzaley A, D'Esposito M. Measuring functional connectivity during distinct stages of a cognitive task. Neuroimage. 2004; 23:752–763. [PubMed: 15488425]

Roberts MJ, Thiele A. Spatial integration and its moderation by attention and acetylcholine. Front. Biosci. 2008; 13:3742–3759. [PubMed: 18508469]

Rogers SL, Farlow MR, Doody RS, Mohs R, Friedhoff LT. A 24-week, double-blind, placebo-controlled trial of donepezil in patients with Alzheimer's disease. Donepezil Study Group. Neurology. 1998; 50:136–145. [PubMed: 9443470]

Rokem A, Landau AN, Garg D, Prinzmetal W, Silver MA. Cholinergic enhancement increases the effects of voluntary attention but does not affect involuntary attention. Neuropsychopharmacology. 2010; 35:2538–2544. [PubMed: 20811340]

Rowan E, McKeith IG, Saxby BK, O'Brien JT, Burn D, Mosimann U, Newby J, Daniel S, Sanders J, Wesnes K. Effects of donepezil on central processing speed and attentional measures in Parkinson's disease with dementia and dementia with Lewy bodies. Dement. Geriatr. Cogn. Disord. 2007; 23:161–167. [PubMed: 17192712]

Rubinov M, Sporns O. Complex network measures of brain connectivity: uses and interpretations. Neuroimage. 2010; 52:1059–1069. [PubMed: 19819337]

Rubinov M, Sporns O. Weight-conserving characterization of complex functional brain networks. Neuroimage. 2011; 56:2068–2079. [PubMed: 21459148]

Rutman AM, Clapp WC, Chadick JZ, Gazzaley A. Early top-down control of visual processing predicts working memory performance. J. Cogn. Neurosci. 2010; 22:1224–1234. [PubMed: 19413473]

Salvador R, Suckling J, Schwarzbauer C, Bullmore E. Unidirected graphs of frequency-dependent functional connectivity in whole brain networks. Philos. Trans. R. Soc. Lond. B Biol. Sci. 2005; 360:937–946. [PubMed: 16087438]

Sarter M, Bruno JP. Trans-synaptic stimulation of cortical acetylcholine and enhancement of attentional functions: a rational approach for the development of cognition enhancers. Behav. Brain Res. 1997; 83:7–14. [PubMed: 9062654]

Sarter M, Hasselmo ME, Bruno JP, Givens B. Unraveling the attentional functions of cortical cholinergic inputs: Interactions between signal-driven and cognitive modulation of signal detection. Brain Res. Brain Res. Rev. 2005; 48:98–111. [PubMed: 15708630]

Sauseng P, Klimesch W. What does phase information of oscillatory brain activity tell us about cognitive processes? Neurosci. Biobehav. Rev. 2008; 32:1001–1013. [PubMed: 18499256]

Sauseng P, Klimesch W, Gruber W, Doppelmayr M, Stadler W, Schabus M. The interplay between theta and alpha oscillations in the human electroencephalogram reflects the transfer of information between memory systems. Neurosci. Lett. 2002; 324:121–124. [PubMed: 11988342]

Sauseng P, Klimesch W, Doppelmayr M, Hanslmayr S, Schabus M, Gruber WR. Theta coupling in the human electroencephalogram during a working memory task. Neurosci. Lett. 2004; 354:123–126. [PubMed: 14698454]

Sauseng P, Klimesch W, Doppelmayr M, Pecherstorfer T, Freunberger R, Hanslmayr S. EEG alpha synchronization and functional coupling during top-down processing in a working memory task. Hum. Brain Mapp. 2005a; 26:148–155. [PubMed: 15929084]

Sauseng P, Klimesch W, Schabus M, Doppelmayr M. Fronto-parietal EEG coherence in theta and upper alpha reflect central executive functions of working memory. Int. J. Psychophysiol. 2005b; 57:97–103. [PubMed: 15967528]

Sauseng P, Klimesch W, Heise KF, Gruber WR, Holz E, Karim AA, Glennon M, Gerloff C, Birbaumer N, Hummel F. Brain oscillatory substrates of visual short-term memory capacity. Curr. Biol. 2009; 19:1846–1852. [PubMed: 19913428]

Schinkel S, Marwan N, Kurths J. Order patterns recurrence plots in the analysis of ERP data. Cogn. Neurodyn. 2007; 1:317–325. [PubMed: 19003502]

Shahaf G, Reches A, Pinchuk N, Fisher T, Ben Bashat G, Kanter A, Tauber I, Kerem D, Laufer I, Aharon-Peretz J, Pratt H, Geva AB. Introducing a novel approach of network oriented analysis of ERPs, demonstrated on adult attention deficit hyperactivity disorder. Clin. Neurophysiol. 2012; 123:1568–1580. [PubMed: 22261156]

Shimamura AP. The role of the prefrontal cortex in dynamic filtering. Psychobiology. 1997; 28:207–218.

Skrandies W. Brain mapping of visual evoked activity-topographical and functional components. Acta Neurol. Taiwan. 2005; 14:164–178. [PubMed: 16425543]

Slagter HA, Kok A, Mol N, Kenemans JL. Spatio-temporal dynamics of top-down control: directing attention to location and/or color as revealed by ERPs and source modeling. Brain Res. Cogn. Brain Res. 2005; 22:333–348. [PubMed: 15722205]

Srinivasan R. Internal and external neural synchronization during conscious perception. Int. J. Bifurc. Chaos. 2004; 14:825–842.

Stam CJ. Nonlinear dynamical analysis of EEG and MEG: review of an emerging field. Clin. Neurophysiol. 2005; 116:2266–22301. [PubMed: 16115797]

Stam CJ, Jones BF, Nolte G, Breakspear M, Scheltens P. Small-world networks and functional connectivity in Alzheimer's disease. Cereb. Cortex. 2007; 17:92–99. [PubMed: 16452642]

Stephane M, Leuthold A, Kuskowski M, McClannahan K, Xu T. The temporal, spatial, and frequency dimensions of neural oscillations associated with verbal working memory. Clin. EEG Neurosci. 2012; 43:145–153. [PubMed: 22715489]

Sun FT, Miller LM, D'Esposito M. Measuring interregional functional connectivity using coherence and partial coherence analyses of fMRI data. Neuroimage. 2004; 21:647–658. [PubMed: 14980567]

Vijayraghavan S, Wang M, Birnbaum SG, Williams GV, Arnsten AF. Inverted-U dopamine D1 receptor actions on prefrontal neurons engaged in working memory. Nat. Neurosci. 2007; 10:376–384. [PubMed: 17277774]

Wesnes KA, McKeith IG, Ferrara R, Emre M, Del Ser T, Spano PF, Cicin-Sain A, Anand R, Spiegel R. Effects of rivastigmine on cognitive function in dementia with Lewy bodies: a randomised placebo-controlled international study using the cognitive drug research computerized assessment system. Dement. Geriatr. Cogn. Disord. 2002; 13:183–192. [PubMed: 11893841]

Wesnes KA, McKeith I, Edgar C, Emre M, Lane R. Benefits of rivastigmine on attention in dementia associated with Parkinson disease. Neurology. 2005; 65:1654–1656. [PubMed: 16301500]

Williams GV, Goldman-Rakic PS. Modulation of memory fields by dopamine D1 receptors in prefrontal cortex. Nature. 1995; 376:572–575. [PubMed: 7637804]

Yener GG, Ba ar E. Sensory evoked and event related oscillations in Alzheimer's disease: a short review. Cogn. Neurodyn. 2010; 4:263–274. [PubMed: 22132038]

Zahrt J, Taylor JR, Mathew RG, Arnsten AF. Supranormal stimulation of D1 dopamine receptors in the rodent prefrontal cortex impairs spatial working memory performance. J. Neurosci. 1997; 17:8528–8535. [PubMed: 9334425]

Zaninotto AL, Bueno OF, Pradella-Hallinan M, Tufik S, Rusted J, Stough C, Pompéia S. Acute cognitive effects of donepezil in young, healthy volunteers. Hum. Psychopharmacol. 2009; 24:453–464. [PubMed: 19637397]

Zanto TP, Gazzaley A. Neural suppression of irrelevant information underlies optimal working memory performance. J. Neurosci. 2009; 29:3059–3066. [PubMed: 19279242]

Zanto TP, Rubens MT, Bollinger J, Gazzaley A. Top-down modulation of visual feature processing: the role of the inferior frontal junction. Neuroimage. 2010; 53:736–745. [PubMed: 20600999]

Zanto TP, Rubens MT, Thangavel A, Gazzaley A. Causal role of the prefrontal cortex in top-down modulation of visual processing and working memory. Nat. Neurosci. 2011; 14:656–661. [PubMed: 21441920]

Zenger B, Braun J, Koch C. Attentional effects on contrast detection in the presence of surround masks. Vis. Res. 2000; 40:3717–3724. [PubMed: 11090664]
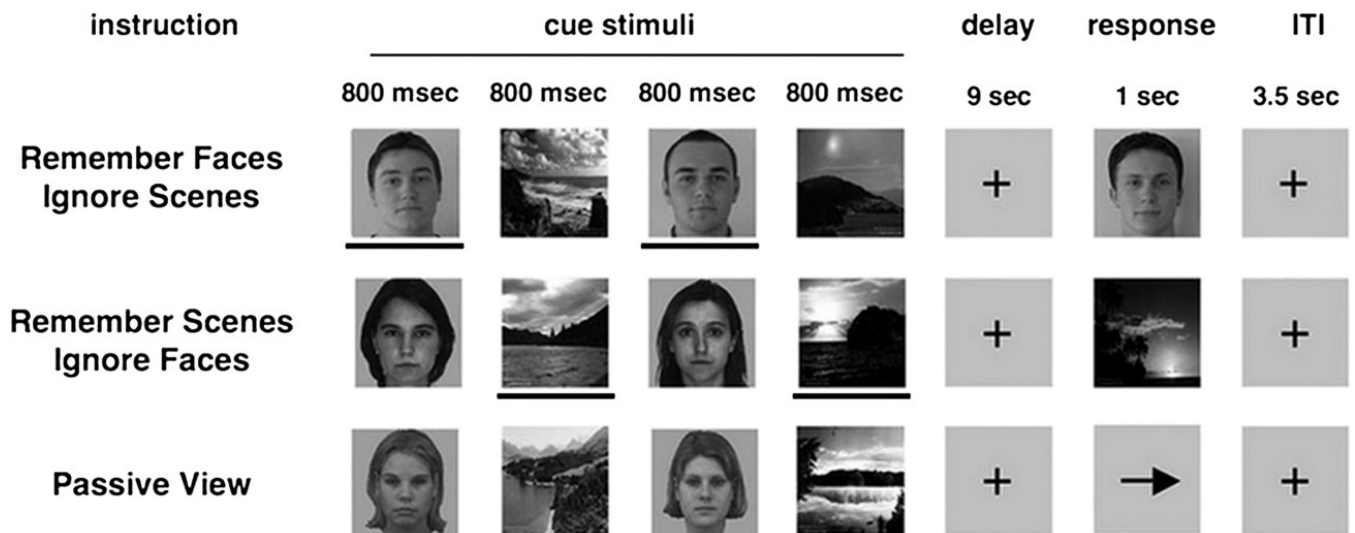
Zhou D, Thompson WK, Siegle G. Matlab toolbox for functional connectivity. Neuroimage. 2009; 47:1590–1607. [PubMed: 19520177]

Fig. 1.
Delay-recognition paradigm. The paradigm consisted of three tasks in which aspects of
visual information were held constant while task-demands were manipulated. During each
trial, participants observed sequences of two faces and two natural scenes (Cue stimuli)
presented in a randomized order. Participants were given the following instructions:
remember faces (ignore scenes, hereafter, Face Memory), remember scenes (ignore faces,
hereafter, Scene Memory) or passively view all stimuli (hereafter, Passive View). The task
was presented in 3 separate runs (20 trials each) with each of the three conditions in
randomorder. Each of the Cue stimuli was presented for a period of 800 ms. After a delay of
9 s. participants were asked to indicate with a button press whether a face or a scene
stimulus (i.e., the probe stimulus, presented for a duration of 1 s)matched the previously
presented relevant cues, yielding performance measures of the WM task (reaction time and
percent-correct). In the passive view response period, an arrow was presented, and
participants were required to make a button press indicating the direction of the arrow. In the
current study, only the electrophysiological responses to the irrelevant distractor face stimuli
appearing in the Cue period of the Scene Memory condition were analyzed. The lines below
the stimuli are used to highlight task-relevance in this illustration and were not present in the
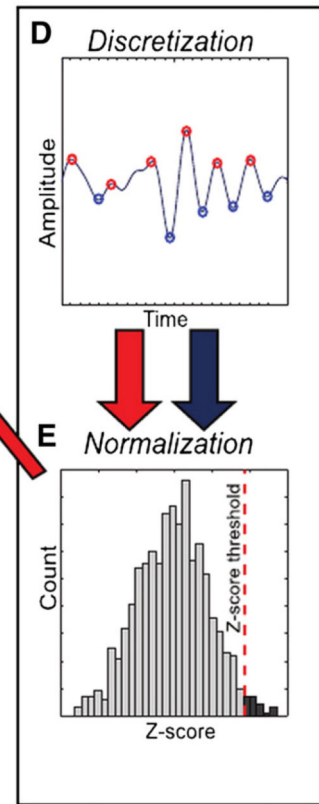actual task. Reproduced from Fig. 1 in Gazzaley et al. (2008).
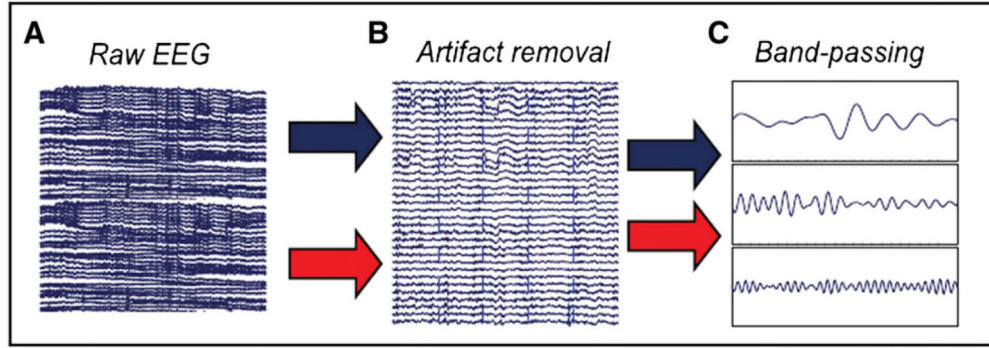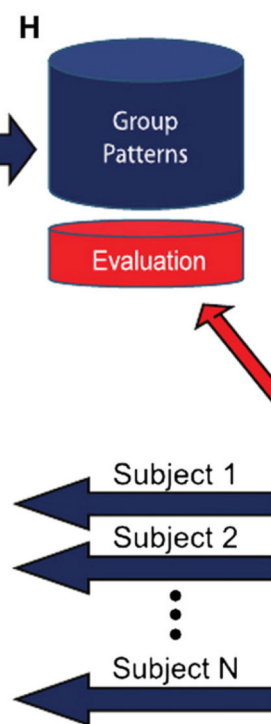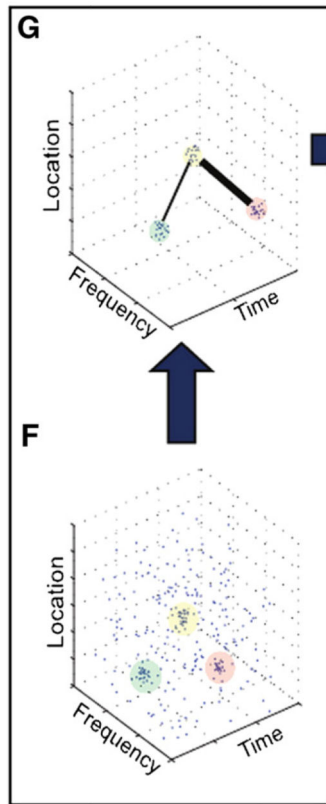
Fig. 2.
Outline of steps in the functional network analysis. The BNA analysis involves two independent processes — group pattern analysis (blue arrows) and individual participant evaluation (red arrows). For the group analysis, the raw EEG of each participant undergoes three separate processing stages: (1) preprocessing (artifact removal, band-passing); (2) salient event extraction (discretization, normalization) and (3) network analysis (unitary event extraction, pair-pattern extraction) on all salient events gathered from all of the participants. The single participant level process involves three stages — the first two are

identical to the first two stages of the group level process. In the third stage, the single participant activity is compared to the set of patterns collected during the group analysis stage. See text for further details. The multiple arrows stemming from the normalization stage represent the pooling of each participant's salient event to form the database on which the pattern analysis stage was performed.

Reproduced from Fig. 1 in Shahaf et al. (2012).
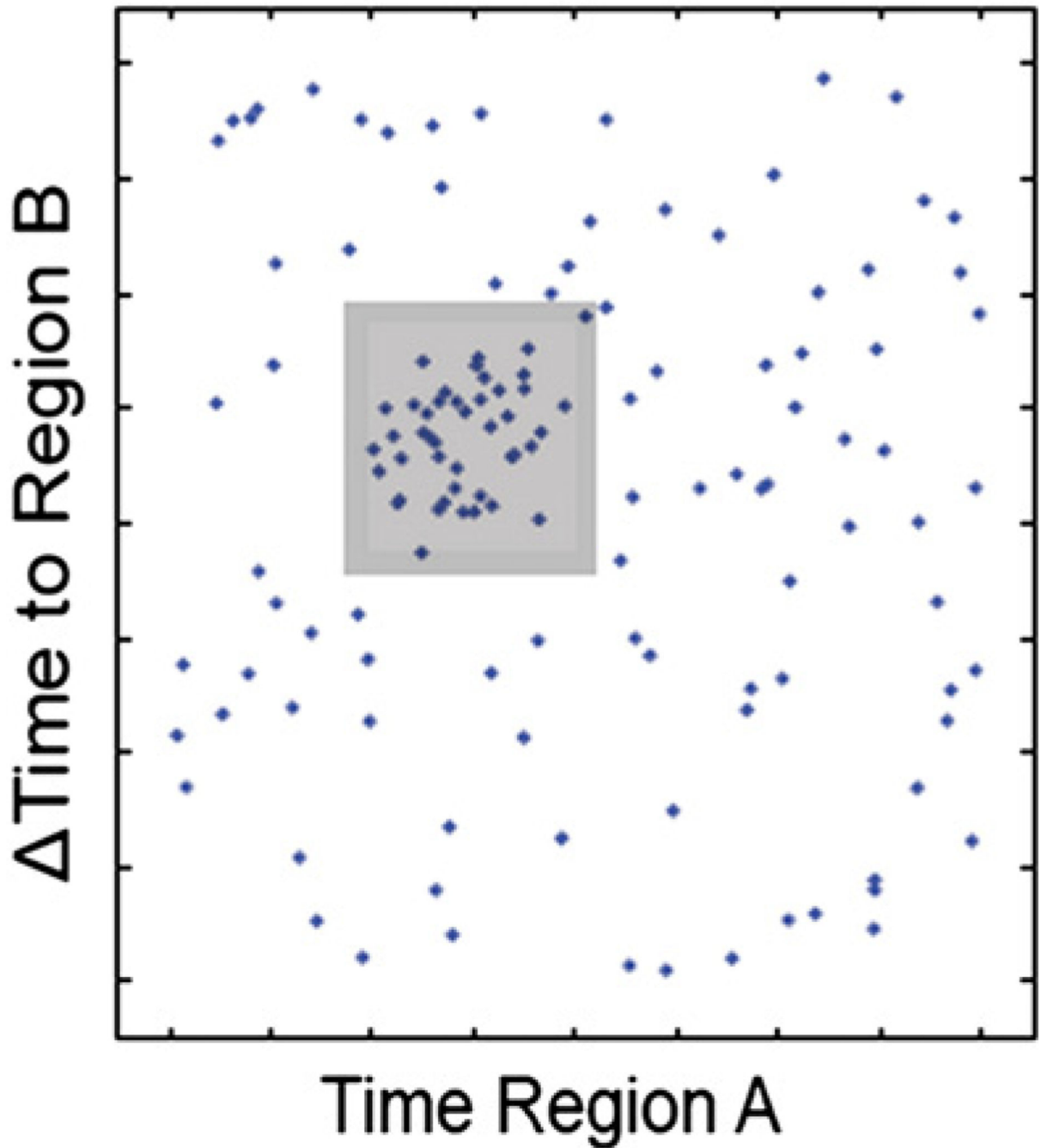
Fig. 3.
Shown is a bi-regional point plane, the X and Y axes of which represent latencies of individual salient events and inter-event intervals, respectively. A sliding adjustable rectangular window searches for clusters containing a minimum number of subjects. A cluster within the plane defines an *event pair* satisfying both absolute and relative time constraints. For further details see text.

Reproduced from Fig. A1 in Shahaf et al. (2012).
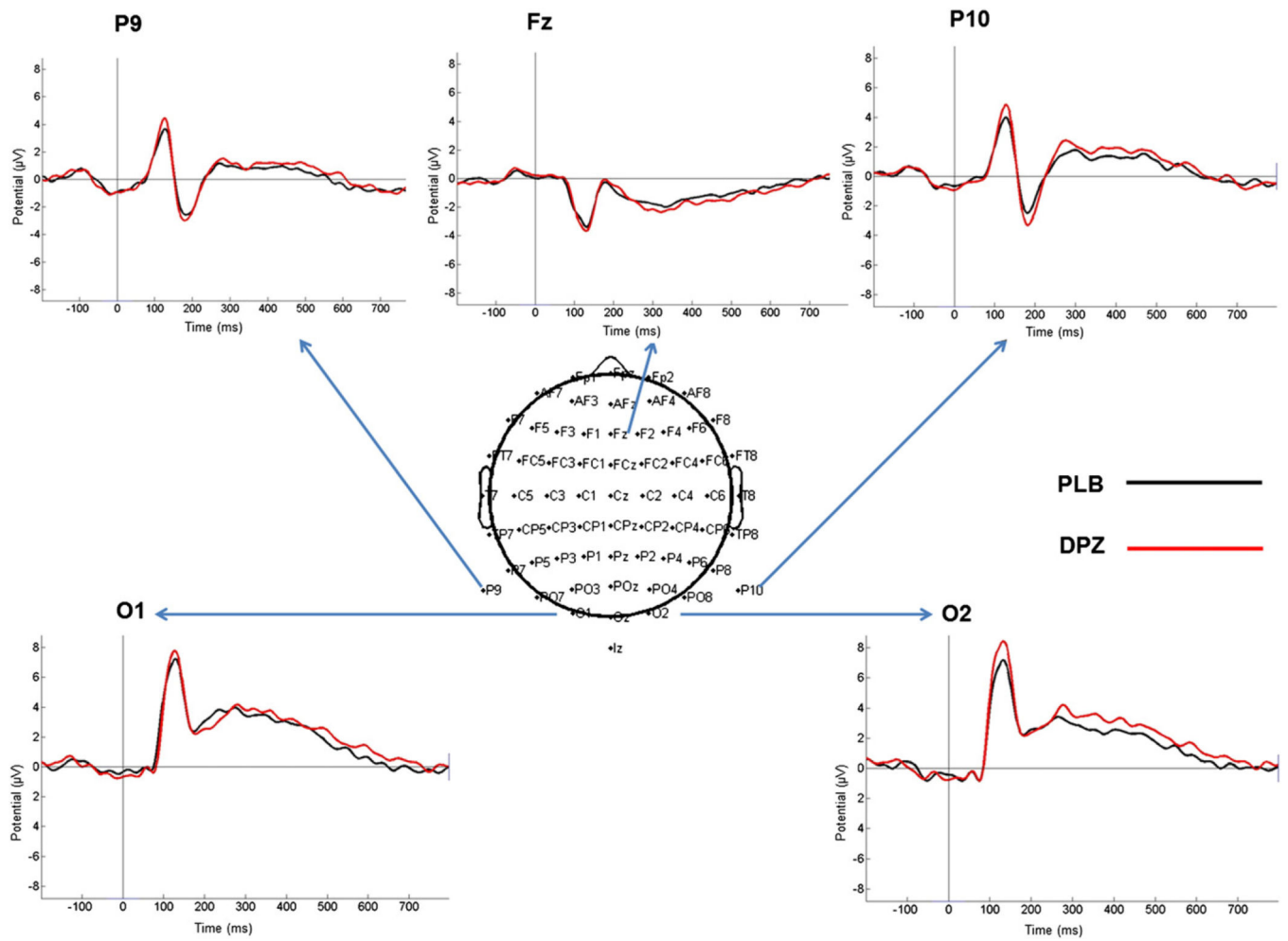
Fig. 4.
Grand-average ERP responses evoked by the irrelevant face stimuli in placebo and donepezil. The middle inset depicts the 64-channel cap (10–20 system) electrode placement (Biosemi Active-two system). For each of the overlaid ERP waveforms the arrows point to the corresponding position of the recording channel. PLB = placebo; DPZ = donepezil.
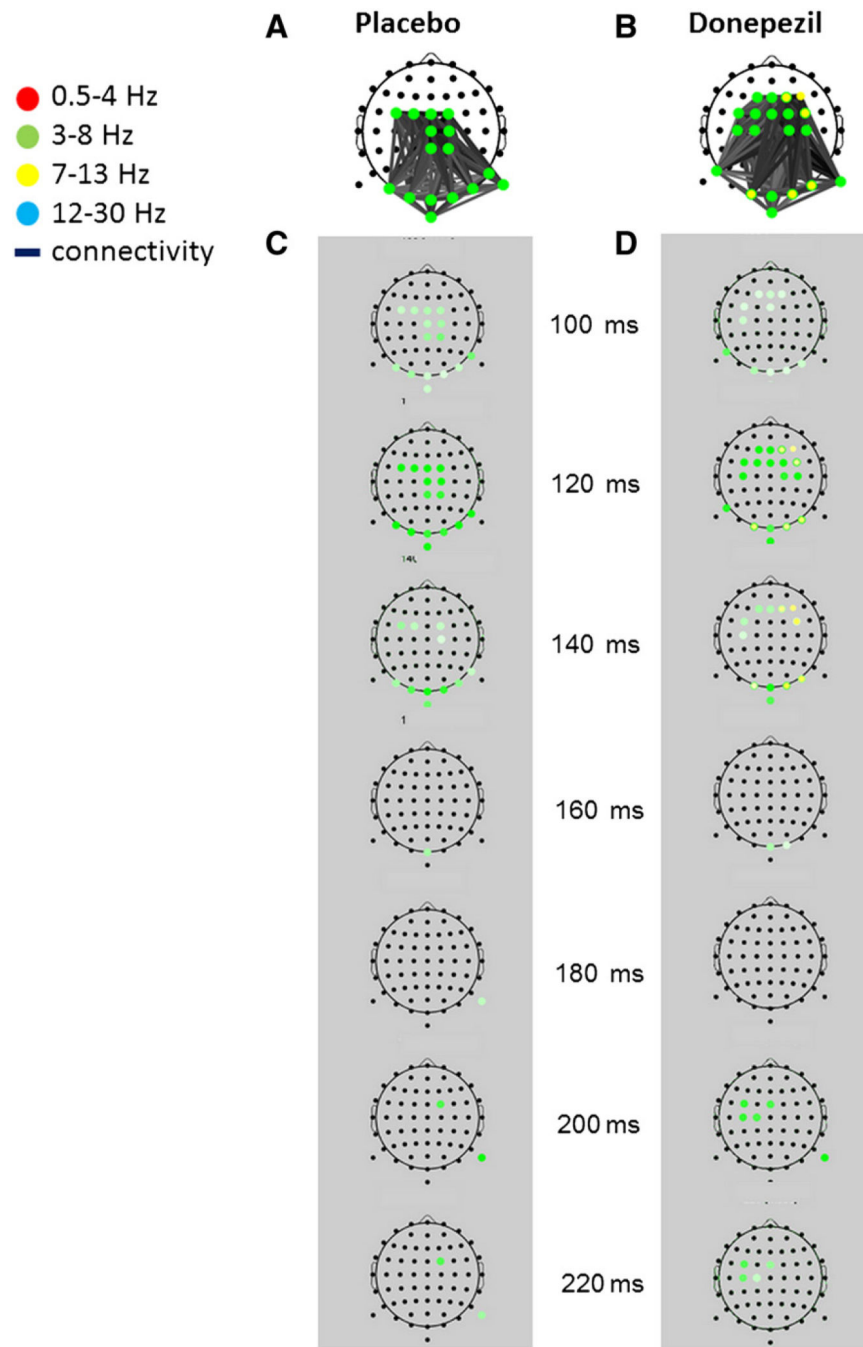
Fig. 5.
BNA networks characterizing the processing of irrelevant faces in placebo (A) and donepezil (B). Upper images (white background) display characteristic network activity overlaid on scalp electrode montage. Discrete time-frame activations depicting the evolution in time (in ms) of each network activation are displayed for placebo and donepezil within the gray background columns beneath each characteristic network (C and D, respectively). A node is represented as a dot on the scalp, while a colored circle at a specific node denotes activity within a specific frequency band/s. The frequency band of the electrode activity is color

coded (see top-left color legend). A colored circle at a node will receive its full hue when the time frame coincides with the group-mean latency of the activity peak and lighter shades when away from it, the spectrum width being dependent on the spread of individual latencies. Gray-shaded lines connect between pair of nodes.

Fig. 6.
Correlations between BNA/sBNA scores and behavioral data. (A) Correlation between BNA scores and performance (under placebo). The graph shows that the donepezil network BNA scores in placebo significantly correlate with performance on the WM task in placebo. (B) The theta–alpha sub-network (sBNA) extracted from the donepezil characteristic network. See colored legend for node activation in Fig. 5. (C) Correlation between sBNA scores and performance improvement. The graph depicts a significant correlation between the donepezil sBNA scores in placebo and the difference of % correct between placebo and donepezil (% correct donepezil-minus-% correct placebo).

Table 1

Mean amplitudes (μV) and latencies (ms) [SD] of the selected components at the electrodes chosen for statistical analysis.

Component		Amplitude				Latency		
		P1	N170	P3	P1	N170	P3	
Electrode		PO3	P10	PO8	PO3	P10	PO8	
Donepezil		5.48 [3.45]	−3.79 [2.51]	6.16 [2.44]	107.76 [27.54]	170.54 [12.05]	386.77 [52.25]	
Placebo		4.89 [3.60]	−2.71 [2.31]	6.05 [3.06]	113.34 [23.79]	174.16 [14.31]	394.31 [52.67]	